



**SYNTHESIS OF RU(II) THIOPHENE-IMIDAZO-PHENANTHROLINE POLYPYRIDYL
COMPLEXES AND THEIR DNA BINDING, PHOTOCLEAVAGE, ANTIMICROBIAL
AND CYTOTOXICITY ACTIVITY PROPERTIES**

A. Dayanand^a, P. Venkat Reddy^a, Ch. Nagamani^a, Y. Praveen Kumar^b, M. Rajender Reddy^a, V. Ravi Kumar^a,
K. Laxma Reddy^a and S. Satyanarayana^{a,*}

^aDepartment of Chemistry, University College of Science, Osmania University, Hyderabad-500007, Telangana State, INDIA.

^bSchool of chemistry, University of Hyderabad-500046, Telangana State, INDIA.

^{*a}Department of Chemistry, University College of Science, Osmania University, Hyderabad-500007, Telangana, INDIA.

***Corresponding Author: Dr. S. Satyanarayana**

Department of Chemistry, University College of Science, Osmania University, Hyderabad-500007, Telangana State, INDIA

Article Received on 07/12/2016

Article Revised on 27/12/2016

Article Accepted on 17/01/2017

ABSTRACT

Six octahedral Ru(II) polypyridyl complexes [Ru(phen)₂NTIP]²⁺ (1), [Ru(bpy)₂NTIP]²⁺ (2), [Ru(dmb)₂NTIP]²⁺ (3), NTIP = 2-(4'-Nitrothiophene)imidazo[4,5-f][1,10]phenanthroline [Ru(phen)₂BTIP]²⁺ (4), [Ru(bpy)₂BTIP]²⁺ (5), [Ru(dmb)₂BTIP]²⁺ (6), BTIP = 2-(4'-Bromo thiophene)imidazo[4,5-f][1,10]phenanthroline; phen = 1,10-phenanthroline; bpy = 2,2'-bipyridine; dmb = 4,4'-dimethyl-2,2'-bipyridine; were synthesized and characterized by Elemental analysis, IR and NMR, Mass spectral methods. Absorption, emission, viscosity titrations were used to investigate the binding of Ru(II) complexes with calf thymus DNA and also investigated photocleavage of plasmid pBR322DNA. Molecular docking studies explored theoretical binding of these complexes. These complexes were assessed for their Antimicrobial and cytotoxic studies.

KEYWORDS: Ru(II) complexes, Photoactivated cleavage, Docking, Antimicrobial and cytotoxicity.

INTRODUCTION

In the development of small molecules as novel reagents for biotechnology and medicine interaction of transition metal complexes with DNA has been the subject of intense investigation.^[1-3] Photochemical, photophysical, photocleavage nature, and DNA structural probe property.^[4-6] molecular light switches.^[7] and photodynamic therapy (PDT).^[8] of Ru (II) polypyridyl complexes have lead to wide applications for them. There are three distinct modes of non covalent interaction of most drugs with DNA, intercalative mode through sliding of a planar, aromatic moiety between DNA base pairs, DNA groove binding by electrostatic, hydrophobic, and hydrogen binding interactions, and external binding involving electrostatic attraction.^[9, 10] Intercalative mode of DNA binding was proved in octahedral Ru (II) complexes.^[11-13] Role of auxiliary ligands was reported by.^[14-17] in Ru(II) complexes for their interaction with DNA. In the spectral properties and DNA interaction auxiliary ligand of ruthenium complexes plays a major role.^[18] though the intercalating ligand in the complex is the polypyridyl ligand but not the ancillary ligand.

Since, last decade our group has been synthesized Ru(II) polypyridyl complexes, and investigated DNA-binding studies.^[19-26] In this paper, we describe the synthesis, characterization, DNA binding studies, antimicrobial and cytotoxicity of ruthenium complexes of [Ru(phen)₂NTIP]²⁺ (1), [Ru(bipy)₂NTIP]²⁺ (2), [Ru(dmp)₂NTIP]²⁺ (3), NTIP = 2-(4'-Nitrothiophene)imidazo[4,5-f][1,10]phenanthroline) [Ru(phen)₂BTIP]²⁺ (4), [Ru(bipy)₂BTIP]²⁺ (5), [Ru(dmp)₂BTIP]²⁺ (6), BTIP = 2-(4'-Bromothiophene)imidazo[4,5-f][1,10]phenanthroline; phen = 1,10-phenanthroline; bpy = 2,2'-bipyridine; dmb = 4,4'-dimethyl-2,2'-bipyridine.

Experimental

Physical Measurements and Materials

IR spectra recorded in KBr discs on a Perkin-FT-IR-1605 spectrophotometer. NMR spectra measured on a Bruker Z Gradient 400 MHz spectrophotometer using DMSO-d₆ as the solvent. UV-Visible spectra recorded with an Elico Biospectrophotometer, model BL 198. Fluorescence spectra recorded with SL 174 spectrofluorometer. Viscosity experiments were carried out on Ostwald Viscometer, immersed in thermostated

water bath maintained at $30 \pm 0.1^\circ\text{C}$. CT-DNA samples approximately 200 base pairs in average length were prepared by sonication in order to minimize the complexities arising from DNA flexibility.

All the solvents were purified before use as per standard procedures. RuCl_3 , 1,10-Phenanthroline, 2,2'-bipyridine, 4,4'-dimethyl-2,2'-bipyridine, 5-nitrothiophene-2-carbaldehyde, 5-bromothiophene-2-carbaldehyde, were purchased from Sigma and other available sources. Supercoiled pBR322 DNA was obtained from Bangalore Genie. The DNA had a ratio of UV absorbance at 260 and 280 nm of 1.8–1.9:1, indicating that the DNA was sufficiently free from protein. DNA concentration per nucleotide was determined by using a molar absorption coefficient [$6,600 \text{ M}^{-1} \text{ cm}^{-1}$] at 260 nm.

Synthesis and characterization

Preparation of the starting materials, ligands and metal complexes: $\text{cis}[\text{Ru}(\text{phen})_2\text{Cl}_2] \cdot 2\text{H}_2\text{O}$, $\text{cis}[\text{Ru}(\text{bpy})_2\text{Cl}_2] \cdot 2\text{H}_2\text{O}$, $\text{cis}[\text{Ru}(\text{dmb})_2\text{Cl}_2] \cdot 2\text{H}_2\text{O}$, NTIP and BTIP [27] were synthesized according to reported procedures. The synthetic route of Ru(II) complexes 1-6 were shown in the Fig 1. Spectral data for all the complexes were tabulated in Table 1 (NMR) and Table 2 (Mass and IR).

Synthesis of $[\text{Ru}(\text{phen})_2\text{NTIP}](\text{ClO}_4)_2 \cdot 2\text{H}_2\text{O}$ (1): A mixture of $\text{cis}[\text{Ru}(\text{phen})_2\text{Cl}_2] \cdot 2\text{H}_2\text{O}$ (0.5mmol) and NTIP (0.5mmol) was heated to reflux in 25 ml ethanol and 15ml of H_2O for 8hrs under Nitrogen atmosphere to give a clear red solution. Upon cooling the solution was treated with a saturated aqueous solution of NaClO_4 to give a red precipitate. The red precipitate was collected and washed with small amounts of water, ethanol and ether and dried under vacuum. Yield: 72%. Anal. calc. For $\text{C}_{41}\text{H}_{29}\text{Cl}_2\text{N}_9\text{O}_{12}\text{RuS}$: C, 47.18; H, 2.80; N, 12.08; Found: C, 47.11; H, 2.69; N, 12.03.

Synthesis of $[\text{Ru}(\text{bpy})_2\text{NTIP}](\text{ClO}_4)_2 \cdot 2\text{H}_2\text{O}$ (2): This complex is prepared by the similar procedure described for the above complex 1 with a mixture of $\text{cis}[\text{Ru}(\text{bpy})_2\text{Cl}_2] \cdot 2\text{H}_2\text{O}$ (0.5mmol) and NTIP (0.5mmol). Yield: 76%. Anal. calc. For $\text{C}_{37}\text{H}_{29}\text{Cl}_2\text{N}_9\text{O}_{12}\text{RuS}$: C, 44.63; H, 2.94; N, 12.66; Found: C, 44.42; H, 2.88; N, 12.55.

Synthesis of $[\text{Ru}(\text{dmb})_2\text{NTIP}](\text{ClO}_4)_2 \cdot 2\text{H}_2\text{O}$ (3): This complex is prepared by the similar procedure described for the above complex 1 with a mixture of $\text{cis}[\text{Ru}(\text{dmb})_2\text{Cl}_2] \cdot 2\text{H}_2\text{O}$ (0.5mmol) and NTIP (0.5mmol).

Yield: 71%. Anal. calc. For $\text{C}_{41}\text{H}_{37}\text{Cl}_2\text{N}_9\text{O}_{12}\text{RuS}$: C, 46.82; H, 3.55; N, 11.98; Found: C, 46.77; H, 3.51; N, 11.75.

Synthesis of $[\text{Ru}(\text{phen})_2\text{BTIP}](\text{ClO}_4)_2 \cdot 2\text{H}_2\text{O}$ (4): This complex is prepared by the similar procedure described for the above complex 1 with a mixture of $\text{cis}[\text{Ru}(\text{phen})_2\text{Cl}_2] \cdot 2\text{H}_2\text{O}$ (0.5mmol) and BTIP (0.5mmol). Yield: 74%. Anal. calc. For $\text{C}_{41}\text{H}_{29}\text{BrCl}_2\text{N}_8\text{O}_{10}\text{RuS}$: C, 45.70; H, 2.71; N, 10.40; Found: C, 45.59; H, 2.70; N, 10.33.

Synthesis of $[\text{Ru}(\text{bpy})_2\text{BTIP}](\text{ClO}_4)_2 \cdot 2\text{H}_2\text{O}$ (5): This complex is prepared by the similar procedure described for the above complex 1 with a mixture of $\text{cis}[\text{Ru}(\text{bpy})_2\text{Cl}_2] \cdot 2\text{H}_2\text{O}$ (0.5mmol) and BTIP (0.5mmol). Yield: 72%. Anal. calc. For $\text{C}_{37}\text{H}_{29}\text{BrCl}_2\text{N}_8\text{O}_{10}\text{RuS}$: C, 43.16; H, 2.84; N, 10.88; Found: C, 43.09; H, 2.72; N, 10.65.

Synthesis of $[\text{Ru}(\text{dmb})_2\text{BTIP}](\text{ClO}_4)_2 \cdot 2\text{H}_2\text{O}$ (6): This complex is prepared by the similar procedure described for the above complex 1 with a mixture of $\text{cis}[\text{Ru}(\text{dmb})_2\text{Cl}_2] \cdot 2\text{H}_2\text{O}$ (0.5mmol) and BTIP (0.5mmol). Yield: 74%. Anal. calc. For $\text{C}_{41}\text{H}_{37}\text{BrCl}_2\text{N}_8\text{O}_{10}\text{RuS}$: C, 45.36; H, 3.43; N, 10.32; Found: C, 45.14; H, 3.27; N, 10.13.

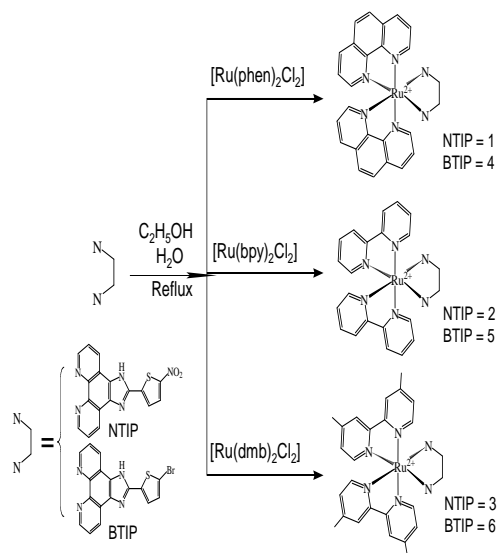


Fig 1. The synthetic route for Ruthenium polypyridyl complexes 1-6.

Table 1: ^1H and ^{13}C -NMR data of Ru(II) complexes 1-6.

Compound	Complexes ^1H NMR data (400 MHz, DMSO- d_6 , TMS)	Complexes ^{13}C [^1H]NMR data (100 MHz, DMSO- d_6 , Major peaks)
1	7.8 (d, 1H), 6.9 (d, 1H), 7.3 (t, 4H), 7.5 (t, 2H), 7.6 (s, 4H), 8 (d, 4H), 8.3 (d, 2H), 8.6 (4H), 8.4 (d, 2H),	121.5, 122.9, 124.2, 126.3, 127.5, 129, 130, 136.4, 141.5, 148, 150, 150.9, 152.9
2	6.8 (d, 1H) 7.7 (d, 1H), 7.2 (t, 2H), 7.4 (t, 4H), 7.1 (t, 4H), 8.7(d, 2H), 8.5(d, 4H), 8 (d, 2H), 8.6(d, 4H)	120.8, 121.5, 122.9, 124.2, 126.1, 126.5, 129, 137.2, 141.5, 148, 150, 151.2, 157.4

3	7.7(d, 1H), 6.8(d, 1H), 8.2(d, 2H), 7.2(t, 2H), 8.9(d, 2H), 8.7(d, 4H), 7.1(d, 4H), 8.4(d, 4H), 2.29 (-CH ₃ , 12H),	24.2, 121.5, 136.4, 127.6, 129.1, 139, 142.5, 146, 152, 153.2, 157.4
4	7.9 (d,1H), 6.9 (d, 1H), 7.2 (t, 4H), 7.5 (t, 2H), 7.7 (s, 4H), 8 (d, 4H), 8.3 (d, 2H), 8.6 (4H), 8.5 (d, 2H),	121.2, 111.8, 121.9, 146.4, 141.6, 124.2, 122.9, 136.4, 126.3, 129, 127.5, 121.5, 148, 150
5	6.8 (d, 1H) 7.7 (d, 1H), 7.2 (t, 2H), 7.4 (t, 4H), 7.1 (t, 4H), 8.6(d, 2H), 8.5(d, 4H), 8 (d, 2H), 8.6(d, 4H)	121.3, 121.9, 122.6, 123.2, 127.1, 129.7, 138.2, 142.5, 144, 150.5, 151.4, 158.7
6	7.7(d, 1H), 6.7(d, 1H), 8.2(d, 2H), 7.2(t, 2H), 8.6(d, 2H), 8.7(d, 4H), 7.0(d, 4H), 8.4(d, 4H), 2.31(-CH ₃ , 12H),	24.6, 121.3, 111, 122, 125.2, 122.9, 126.3, 127.5, 129, 136.4, 141.9, 146.7, 148, 150.5, 125.3, 157.9, 148.5

Table 2: FTIR (cm⁻¹) and Mass data of Ru(II) complexes 1-6.

Compound	FTIR (KBr, cm ⁻¹)	ESI-MS(CH ₃ -CN, m/z)
1	1622 (C = N), 3075, (C-H), 1556 (C = C), 623 (Ru-N), 1190 (N-C), 1235 (C-C).	cal: 809; found: 810.
2	1614 (C = N), 3073 (C-H), 1554 (C = C), 625 (Ru-N), 1185 (N-C), 1253 (C-C).	cal: 761; found: 762.
3	1621 (C = N), 3090 (C-H), 1515 (C = C), 628 (Ru-N), 1171(N-C), 1234 (C-C).	cal: 817; found: 818.
4	1604 (C = N), 3101, (C-H), 1541 (C = C), 620 (Ru-N), 1200 (N-C), 1242 (C-C).	cal: 842; found: 843.
5	1616 (C = N), 3171 (C-H), 1565 (C = C), 625 (Ru-N), 1102 (N-C), 1209 (C-C).	cal: 794; found: 795.
6	1625 (C = N), 3121, (C-H), 1527 (C = C), 626 (Ru-N), 1200 (N-C), 1261 (C-C).	cal: 851; found: 852.

DNA binding studies

The UV-visible absorption titrations of the complexes, both in the absence and presence of CT-DNA, at room temperature in tris-buffer were performed by titrating fixed concentration of complex, to which increments of the DNA stock solution were added. Ru-DNA solutions were allowed to incubate for 5min before recording the absorption spectra. In order to evaluate the binding strength of the complex, the intrinsic binding constant K_b , with CT-DNA was obtained by monitoring the change in the absorbance at metal to ligand charge transfer (MLCT) band, with increasing concentration of DNA. The intrinsic binding constant K_b , of the Ru(II) complexes bound to DNA was calculated from Equation [28]. $[DNA]/(\epsilon_a - \epsilon_f) = [DNA]/(\epsilon_b - \epsilon_f) + 1/K_b (\epsilon_b - \epsilon_f)$ where, [DNA] is the concentration of DNA. The apparent extinction coefficient (ϵ_a) was obtained by calculating $A_{obs}/[Ru]$. The terms ϵ_f and ϵ_b correspond to the extinction coefficients of free (unbound) and the fully bound complex respectively. From plot of $[DNA]/(\epsilon_a - \epsilon_f)$ against [DNA] will give a slope $1/(\epsilon_b - \epsilon_f)$ and an intercept $1/K_b(\epsilon_b - \epsilon_f)$, K_b is the ratio of the slope to the intercept.

In the Fluorescence emission titrations fixed metal complex concentration was taken, to which varying concentration of DNA was added. The excitation wavelength was taken fixed and the emission range was adjusted before measurements. The fraction of the ligand bound was calculated from the relation $C_b = C_t[(F - F_0)/(F_{max} - F_0)]$, where C_t is the total complex concentration, F is the observed fluorescence emission intensity at a given DNA concentration, F_0 is the

intensity in the absence of DNA, and F_{max} is when complex is fully bound to DNA. Binding constant (K_b) was obtained from a Scatchard plot of r/C_f against r , where r is the $C_b/[DNA]$ and C_f is the concentration of free complex.

Fluorescence quenching experiments of complexes were carried out in the absence and presence of DNA with varying concentration of $[Fe(CN)_6]^{4-}$ as quencher. The Stern-Volmer quenching constant (K_{sv}) can be determined by using Stern-Volmer equation.^[29] $I_0/I = 1 + K_{sv} [Q]$, where I_0 and I are the intensities of the fluorophore in the absence and presence of quencher respectively, Q is the concentration of the quencher, and K_{sv} is a linear Stern-Volmer quenching constant.

Viscosity experiments were carried out with an Ostwald viscometer, placed in a thermostatic water bath to maintain at a constant temperature 30.0 ± 0.1 °C. Calf thymus DNA samples approximately 200 base pairs were prepared by sonicating in order to minimize complexities arising from DNA flexibility. Flow time was measured with a digital stopwatch and each sample was measured three times, and then an average flow time was calculated. Data were presented as $(\eta/\eta_0)^{1/3}$ versus the $[complex]/[DNA]$, where η is the viscosity of DNA in presence of complex and η_0 is the viscosity of DNA alone. Viscosity values were calculated from the observed flow time of DNA-containing solutions ($t > 100$ s) corrected for the flow time of the buffer alone (t_0).^[30]

The cleavage of DNA was performed by using agarose gel electrophoresis experiments. In this experiment supercoiled pBR322 DNA (100 μM) was treated with two different concentrations of Ru(II) complexes (40 and 80 μM) and the samples were then irradiated at room temperature with a UV lamp (365 nm) for 30 minutes. Samples were analyzed by electrophoresis for 1 h at 90 V on a 0.8% agarose gel in Tris–acetic acid–EDTA buffer (1X TAE buffer). The gel was stained with 1 $\mu\text{g}/\text{ml}$ ethidium bromide and then photographed under UV light.

The antimicrobial of complexes 1-6 were performed against standard gram positive (*B.Subtilis*, *S.aureus*, *S.epidermidis*) gram negative (*E.coli*, *P.aeroginosa*, *K.pneumoniae*) microorganisms using disc diffusion method.^[31] The Mueller Hinton agar was prepared and poured fresh into sterile Petri plates, and inoculate 0.2 mL of bacterial culture which has 10^6 cells/mL concentrations. Filter paper discs approximately 5mm in diameter were placed in the previously prepared agar plates. Each plate contains standard microorganisms with 5 μL three different complexes (100 μM) and the agar plates were then incubated at 37°C. After 24 hrs of incubation, the resulting zones of inhibition were uniformly circular with a confluent lawn of growth. The diameters of the zones of inhibition were measured (in mm), including the diameter of the disc where the DMSO and Streptomycin used as negative and positive controls, respectively. The minimum inhibitory concentrations (MICs) for these complexes were measured.

To determine cell viability, standard 3-(4,5-dimethylthiazole)-2,5-diphenyltetrazolium bromide (MTT) assay procedures were used [32]. HeLa cells were placed in 96-well micro assay culture plates (8×10^3 cells per well) and grown overnight at 37 °C in a 5% CO₂ incubator. The complexes tested were dissolved in DMSO and diluted with RPMI 1640 and then added to the wells to achieve final concentrations ranging from 10^{-6} to 10^{-4} M. Control wells were prepared by addition of culture medium (100 μL). Wells containing culture medium without cells were used as blanks. The plates were incubated at 37 °C in a 5% CO₂ incubator for 48 h. Upon completion of the incubation, stock MTT dye solution (20 μL , 5 mg/mL) was added to each well. After 4h, buffer (100 μL) containing N, N-dimethylformamide (50%) and sodium dodecyl sulfate (20%) was added to solubilize the MTT formazan. The optical density of each well was then measured on a microplate spectrophotometer at a wavelength of 490 nm. The IC₅₀ values were determined by plotting the percentage of cell viability against concentration of complex graph and reading the concentration at which 50% of cells remain viable relative to the control. Each experiment was repeated at least three times to get the mean values.

The DNA crystal structure was downloaded from protein data bank (PDB ID: 5J3G) into the MOE (Molecular

Operating Environment) software [33]. All water molecules were removed and all polar hydrogen atoms were added to the DNA structure with their standard geometry followed by energy minimization was applied. The 3D structure of the Ru(II) complexes were drawn using Chemscketch software and saved in Mol2 format, and energy minimized in Discovery Studio. All the complexes were docked into the DNA using MOE. It gives a list of conformations and the best fit into the active site was found based on the interaction energy between DNA and complex. MOE S-score is used to estimate the binding energies of top ranked conformations.

RESULTS AND DISCUSSION

Absorption studies

Electronic absorption spectroscopic titration is an effective method that provides information on DNA-binding strength of small molecules. Complex binding with DNA through intercalation usually results in hypochromism and bathochromism, because of the intercalative mode involving a strong stacking interaction between an aromatic ligands and DNA base pairs. Fig 2 shows that the absorption spectra of complexes 1-6 in the absence and presence of CT-DNA. The bands below 300 nm are attributed to intraligand $\pi \rightarrow \pi^*$ transitions, while the metal to ligand charge transfer (MLCT) bands (metal $d\pi$ orbital to ligand π^* orbital) appear at 435, 447, 453, 441, 445 and 439 nm, for complexes 1, 2, 3, 4, 5 and 6, respectively. The change in absorbance of the MLCT bands with increasing amount of CT-DNA was used to derive the intrinsic binding constants (K_b) [34, 35]. The K_b values were determined 4.45×10^5 , 2.3×10^5 , 1.43×10^5 , 3.21×10^5 , 2.63×10^5 and 1.31×10^5 , for complexes 1, 2, 3, 4, 5 and 6, respectively. The different DNA-binding constants of the Ru(II) complexes 1-6 are due to the difference in the ligands.

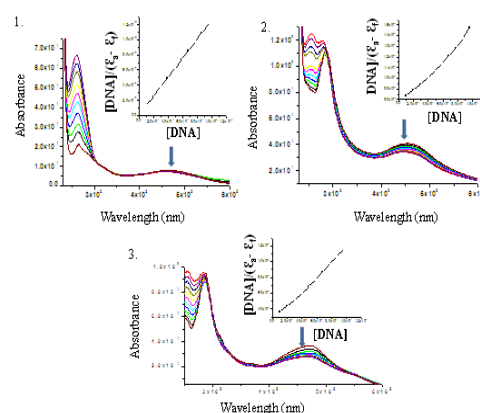


Fig 2. Absorption spectra of complexes 1-3 in Tris-HCl buffer at 25°C upon addition of CT-DNA. [Ru] = 20 μM , [DNA] = 0–120 μM . Arrow shows the absorbance change upon the increase of CT-DNA concentration. Insert: Plots of $[\text{DNA}]/(\epsilon_a - \epsilon_f)$ vs $[\text{DNA}]$ for the titration of DNA with Ru(II) complexes.

Fluorescence spectroscopic studies

The DNA binding abilities of Ru(II) complexes 1-6, were further investigated by fluorescence titration measurements. Changes in emission spectra of the complexes 1–6 in the absence and in the presence of CT-DNA are shown in Fig 3. At their MLCT band excitation, all the complexes emit relatively moderate emission in the absence of DNA in tris buffer at room temperature with the emission maxima at 596–620 nm. Upon addition of CT-DNA to complex the fluorescence emission intensities of complexes 1, 2, 3, 4, 5 and 6, increased by a factor of 4.1, 2.8, 2.4 3.0, 2.3, and 2.0 times, respectively. Scatchard plots for complexes have been constructed from fluorescence emission spectra and binding constants (K_b) for complexes 1, 2, 3, 4, 5 and 6 were found 5×10^5 , 4×10^5 , 2×10^5 , 4×10^5 , 3×10^5 and 1×10^5 , respectively. This indicates that all the complexes can strongly interact with DNA and be protected by the hydrophobic environment inside the DNA helix.

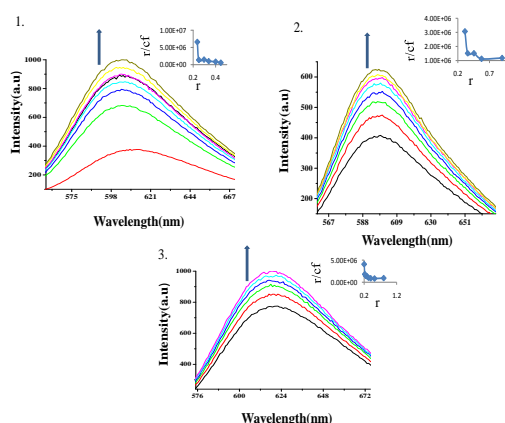


Fig 3. Emission spectra of complexes 1-3 in Tris-HCl buffer at 25°C upon addition of CT-DNA, [Ru] = 20 μM, [DNA] = 0–120 μM. The arrow shows the

Table 3: Quenching data of complexes 1-6.

Compound	Complex alone	Complex: DNA	
		1:30	1:100
1	4372	970	254
2	2853	1263	932
3	2348	1624	1126
4	3623	1198	392
5	3105	2314	892
6	2541	1724	1092

Viscosity measurements

The mode of interaction between the complexes and CT-DNA can be determined by viscosity measurements. Photophysical probes provide necessary, but not sufficient, clues to support a binding model. A hydrodynamic measurement such as viscosity is sensitive to change in length and is regarded as the least ambiguous and most critical tests of a binding model. In classical intercalation, the DNA helix lengthens as base pairs are separated to accommodate the bound ligand leading to an increase in the viscosity of the DNA solution [38]. The effects of complexes 1-6 and Ethidium

increase in intensity upon increasing CT-DNA concentrations.

Quenching studies

Emission quenching experiments gives further support about binding of ruthenium complex with DNA. $[\text{Fe}(\text{CN})_6]^{4-}$ used as anion quencher to observe the binding of complexes with CT-DNA. Fig 4 shows the Stern–Volmer plots for the free complex in solution has high K_{sv} than in the presence of DNA. Highly negatively charged quencher is expected to be repelled by the negatively charged phosphate backbone, and therefore a DNA bound cationic complex should be less quenched by anionic quencher, than the unbound complex [36, 37]. All the complexes show linear Stern–Volmer plots. The K_{sv} value for the complexes in absence of DNA and in the presence of DNA (1:30 and 1:100) with $[\text{Fe}(\text{CN})_6]^{4-}$ given in (Table 3).

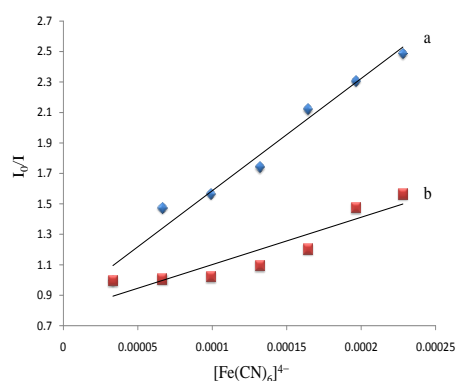


Fig 4. Emission quenching of complex 1 with increasing $[\text{Fe}(\text{CN})_6]^{4-}$ In the absence of DNA (a) and presence of DNA and 1:100 (b).

Bromide on the viscosity of rod like DNA are shown in Fig 5. As the concentration of the complexes increases, the relative viscosity of DNA increases, it indicates that all the complexes 1-6 bind to DNA through intercalation and the difference in the binding strength may be caused by the different ligands.

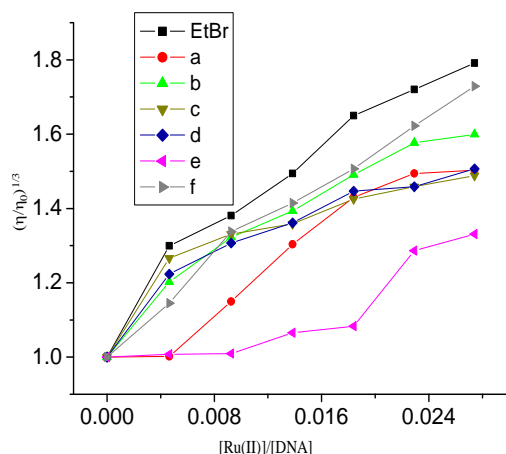


Fig 5. Effect of increasing amount of ethidium bromide, complex 1(c), 2(b), 3(a), 4(d), 5(e) and 6(f) on relative viscosity of CT-DNA at $30 \pm 0.1^\circ\text{C}$. The total concentration of DNA is 0.25 mM.

Photocleavage of pBR322 DNA

After establishing the binding abilities of Ru(II) complexes with DNA, the photocleavage experiments were performed by agarose gel electrophoresis using plasmid DNA (pBR322 DNA) irradiated at 365 nm for 30 minutes. The pBR322 plasmid DNA can exist in three different forms supercoiled, nicked, and linear. These three different forms can be distinguished by gel electrophoresis. When circular plasmid DNA is subjected to electrophoresis, relatively fast migration will be observed in the intact supercoiled form (Form I) [39, 40]. If one strand is cleaved, the supercoil will relax to generate a slower moving open circular form (Form II). If both strands are cleaved, a linear form (Form III) that migrates between Form-I and Form-II will be generated. In the present studies cleavage reactions on plasmid DNA induced with different concentrations of Ru(II) complexes 1-6 (20 and 40 μM) were performed and monitored by agarose gel electrophoresis (Fig 6). With

increasing concentration of Ru(II) complexes the amount of form-I pBR322 DNA was diminished gradually, whereas Form-II increases and Form-III is also produced.

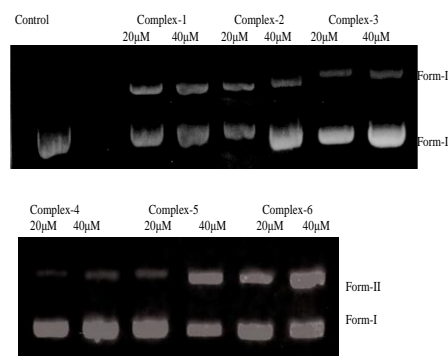


Fig 6. Agarose gel electrophoresis of pBR322 DNA in the presence of different concentrations (20 μM , and 40 μM) of complexes 1-6 after irradiation at 365 nm for 30 min.

Antimicrobial activity of complexes

All the synthesized complexes were tested for in vitro antimicrobial activity. The MIC values of the complexes 1-6 against gram positive (*B.Subtilis*, *S.aureus*, *S.epidermidis*) and gram negative (*E.coli*, *P.aeruginosa*, *K.pneumoniae*) microorganisms were given in Table 4. The experimental results of antimicrobial activity indicated a variable degree of efficacy of the compounds against different strains of bacteria. Streptomycin and DMSO were used as positive and negative controls, respectively. It is found that these Ruthenium polypyridyl complexes are having anti bacterial activity but does not possess significant antifungal activity.

Table 4 The MIC values of the complexes 1-6.

Compound	MIC ($\mu\text{g/ml}$)					
	<i>B.Subtilis</i>	<i>S.aureus</i>	<i>S.epidermidis</i>	<i>E.coli</i>	<i>P.aeruginosa</i>	<i>K.pneumoniae</i>
1	37.5	9.375	37.5	18.75	37.5	75
2	37.5	75	>150	>150	>150	>150
3	75	150	150	75	150	>150
4	>150	>150	>150	>150	>150	>150
5	>150	>150	>150	>150	>150	>150
6	>150	>150	>150	>150	>150	>150
Streptomycin	6.25	6.25	3.125	6.25	1.562	3.125

In vitro cytotoxicity assay

The cytotoxicity of all six complexes against HeLa cell lines was evaluated by MTT assay. Cisplatin and DMSO used as positive and negative controls, respectively. After treatment of HeLa cell line for 48 h with complexes 1-6 in the range of concentrations (4-100 μM). The inhibitory percentage against growth of cancer cells was determined. The cytotoxicity of complexes was found to be concentration-dependent. The cell viability

decreased with increasing the concentrations of complexes 1-6 (Fig 7). The IC_{50} values of complexes 1, 2, 3, 4, 5, 6 and Cisplatin were 42.52 ± 0.5 , 49.46 ± 0.5 , 63.84 ± 0.5 , 48.52 ± 0.5 , 69.46 ± 0.5 , 70.25 ± 0.5 and $4.80 \pm 0.5 \mu\text{M}$, respectively.

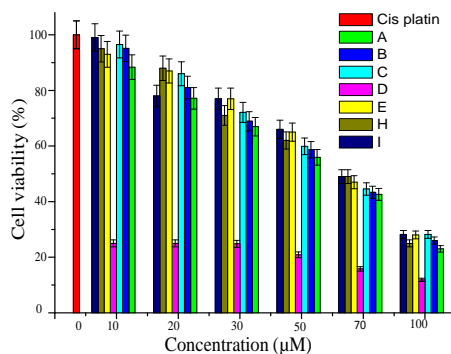


Fig 7. Cytotoxicity of Hela cell lines in vitro treatment with complexes 1-6. Each data point is the mean \pm standard error obtained from at least three independent experiments.

Docking studies

Molecular docking was performed to further explore the binding affinity of complex with DNA. The best pose was selected and used for further study. Docking results indicated that Ru(II) complexes bind with DNA molecule through hydrogen bonds and Vander Waals interactions, which can be evaluated very rapidly during the docking process. Hydrogen bonds play an important role for the interaction of complex with DNA. It is clear

that all the complexes were bound into the binding cavity of DNA making interactions with the Base pairs. Receptor Interacting residues, S-Score and Hydrogen bond distance for all complexes were tabulated in Table 5. Fig 8 showed interactions between complex and DNA.

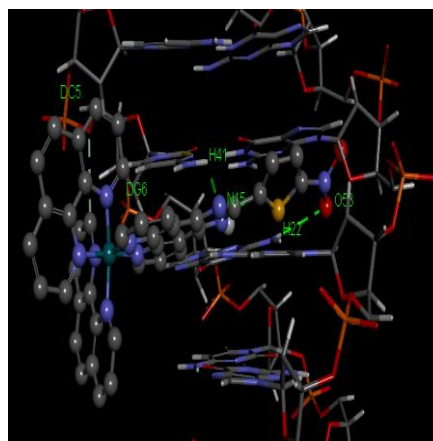


Fig 8. Interactions between complex 1 and DNA (PDB ID: 5J3G).

Table 5 Interacting residues, S-Score and Hydrogen bond distance of complexes 1-6.

Compound	S- Score	Interacting residues	Hydrogen Bond distance(Å)
1	-8.5562	A:DC5:H41 – Molecule:N15 A:DG6:H22 – Molecule:O53	1.88 2.01
2	-8.6316	B:DG16:H21 – Molecule:N39 B:DG16:H22 – Molecule:O50	2.31 3.17
3	-7.6130	A:DC5:O2 – Molecule:H75	2.82
4	-7.6978	B:DG16:H21 – Molecule:N43	1.94
5	-6.0258	A:DC5:O2 – Molecule:H71	2.74
6	-6.7595	A:DC5:O2 – Molecule:H71	2.64

CONCLUSIONS

Six Ru(II) polypyridyl complexes have been synthesized and characterized. The DNA-binding properties of all the six complexes with CT-DNA were investigated by spectroscopic titrations and viscosity measurements. The results revealed that these complexes can intercalate into DNA base pairs. Molecular docking studies were also used to explore the binding affinities of ruthenium complexes. All the synthesized complexes can effectively cleave plasmid DNA, and exhibit good antimicrobial activity against *B.Subtilis*, *S.aureus*, *S.epidermidis*, *E.coli*, *P.aeruginosa*, *K.pneumoniae*. *In vitro* cytotoxicity assay showed that these ruthenium complexes have antitumor activity but less than that of positive control cisplatin against HeLa cell lines

ACKNOWLEDGMENTS

We are grateful to the UGC SERO Hyderabad INDIA, BJR GDC Osmania University, Hyderabad Telangana State INDIA, DST-SERB New Delhi, and we are also grateful to UGC New Delhi and to CFRD, Osmania University, Hyderabad, Telangana, INDIA.

REFERENCES

- Chao Tua, Xuefeng Wub, Qin Liua, Xiaoyong Wang, Qiang Xub, Zijian Guoa. Crystal structure, DNA-binding ability and cytotoxic activity of platinum(II) 2,2'-dipyridylamine complexes. *J Inorg Chim Acta*, 2004; 357: 95–102.
- Chowdhury SR, Mukherjea KK, Bhattacharyya R. Biophysical and biochemical investigation on the binding of a manganese-cyanonitrosyl complex with DNA. *J Trans Metal Chem*, 2005; 30: 601–604.
- Yu-min Sng, Xiao-lin Lu, Mei-ling Yang, Xiu-rong Zheng. Study on the interaction of platinum(IV), gold(III) and silver(I) ions with DNA. *Trans Metal Chem*, 2005; 30: 499–502.
- Erkkila KE, Odom DT, Barton JK. Recognition and reaction of metallointercalators with DNA. *Chem Rev*, 1999; 99: 2777–2795.
- Metcalf C, Thomas JA. Kinetically inert transition metal complexes that reversibly bind to DNA. *Chem Soc Rev*, 2003; 32: 215–224.
- Ya Xiong, Liang-Nian Ji, Synthesis, DNA-binding and DNA-mediated luminescence quenching of

- Ru(II) polypyridine complexes, *Chem Rev*, 1999; 711: 185–191.
- Friedman AE, Chambron JC, Sauvage JP, Turro NJ, Barton JK, A molecular light switch for DNA: [Ru(bpy)₂(dppz)]²⁺. *J Am Chem Soc*, 1990; 112: 4960–4962.
 - Sandya Rani-Beeram, Kyle Meyer, Anna McCrate, Yiling Hong, Mark Nielsen Shawn Swavey, A Fluorinated Ruthenium Porphyrin as a Potential Photodynamic Therapy Agent: Synthesis, Characterization, DNA Binding, and Melanoma Cell Studies. *Inorg Chem* 2008; 47: 11278–11283.
 - Hwa-Yun B, Hee-Jeon S, Cho TS, Yoon YS, Sehlstedt U, Kim SK, Binding mode of porphyrins to poly[d(A-T)₂] and poly[d(G-C)₂]. *J Biophys Chem*, 1998; 70: 1-10.
 - Tan JH, Lu YJ, Huang Zh Sh, Gu LQ, Wu JY, Stabilization of G-quadruplex DNA and down-regulation of oncogene c-myc by quindoline derivatives. *Eur J Med Chem*, 2007; 50: 1465–1474.
 - Pierroz V, Joshi T, Leonidova A, Mari C, Schur J, Ott I, Spiccia L, Ferrari S, Gasser G, Molecular and cellular characterization of the biological effects of ruthenium(II) complexes incorporating 2-pyridyl-2-pyrimidine-4-carboxylic acid. *J Am Chem Soc*, 2012; 134: 20376–20387.
 - Huang HL, Li ZZ, Liang ZH, Liu YJ, Cell Cycle Arrest, Cytotoxicity, Apoptosis, DNA-Binding, Photocleavage, and Antioxidant Activity of Octahedral Ruthenium(II) Complexes. *Eur J Inorg Chem*, 2011; 36: 5538–5547.
 - Liu XW, Li L, Lu JL, Chen YD, Zhang DS, Synthesis, DNA-binding, and photocleavage studies of ruthenium(II) complexes with an asymmetric ligand. *J Coord Chem*, 2011; 64: 4344–4356.
 - Xiong Y., Ji L.N. Synthesis, DNA-binding and DNA-mediated luminescence quenching of Ru(II)polypyridine complexes. *Coord Chem Rev*, 1999; 711: 185–191.
 - Mei JW, Liu J, Zheng KC, Li LJ, Chao Li H, An X, Yun CF, Ji LN, Experimental and theoretical study on DNA-binding and photocleavage properties of chiral complexes Δ- and Λ-[Ru(bpy)₂L](L = o-hpip, m-hpip and p-hpip). *Dalton Trans.*, 2003; 27: 1352–1359.
 - J. G. Liu, Q. L. Zhang, X. F. Shi, and L. N. Ji, “Interaction of [Ru(dmp)₂(dppz)]²⁺ and [Ru(dmb)₂(dppz)]²⁺ with DNA: effects of the ancillary ligands on the DNA-binding behaviors,” *Inorganic Chemistry*. 2001; 40: 5045–5050.
 - Chen LM, Chen JC, Tan CP, Tan CP, Shuo Shi, Zeng KC, Ji LN, Synthesis, characterization, DNA-binding and spectral properties of complexes [Ru(L)₄(dppz)]²⁺ (L = Im and MeIm). *J Inorg Biochem*, 2008; 102: 330–341.
 - Mariappan M, Maiya BG, Effects of Anthracene and Pyrene Units on the Interactions of Novel Polypyridylruthenium(II) Mixed-Ligand Complexes with DNA. *Eur J Inorg Chem*, 2005; 11: 2164–2173.
 - Venkat Reddy P, Nagamani Ch, Rajender Reddy M, Srishailam A, Nagasuryaprasad K, Deepika N, Yaswanth VVN, Prakasham RS, Singh SS, Satyanarayana S. Synthesis and Evaluation of In Vitro DNA/Protein Binding Affinity, Antimicrobial, Antioxidant and Antitumor Activity of Mononuclear Ru(II) Mixed Polypyridyl Complexes. *J Fluoresc.*, 2015; 26: 225–240.
 - Venkat Reddy P, Rajender Reddy M, Srishailam A, Praveen Kumar Y, Nagamani Ch, Deepika N, Nagasuryaprasad K, Singh SS, Satyanarayana S, Design, synthesis, DNA-binding affinity, cytotoxicity, apoptosis, and cell cycle arrest of Ru(II) polypyridyl complexes. *Analy Biochem*, 2015; 485: 49–58.
 - Srishailam A, Gabra NM, Kumar YP, Reddy KL, Shobha Devi C, Kumar DA, Singh SS, Satyanarayana S. Synthesis, characterization; DNA binding and antitumor activity of ruthenium(II) polypyridyl complexes. *J of Photochem and Photobio B*, 2014; 141: 47–58.
 - Reddy MR, Reddy PV, Kumar YP, Srishailam A, Navaneetha N, Satyanarayana S. Synthesis, Characterization, DNA Binding, Light Switch “On and Off”, Docking Studies and Cytotoxicity, of Ruthenium(II) and Cobalt(III) Polypyridyl Complexes. *J Fluoresc*, 2014; 24; 803–817.
 - Devi CS, Nagababu P, Sumathi N, Deepika N, Reddy PV, Veerababu N, Singh SS, Satyanarayana S. Cellular uptake, cytotoxicity, apoptosis and DNA-binding investigations of Ru(II) complexes. *J Fluoresc*, 2014; 72; 160–169.
 - Gabra NM, Mustafa B, Kumar YP, Devi CS, Srishailam A, Reddy PV, Reddy KL, Satyanarayana S, Synthesis, DNA-binding, Cytotoxicity, Photo Cleavage, Antimicrobial and Docking Studies of Ru(II) Polypyridyl Complexes. *J Fluoresc*, 2014; 24; 169–181.
 - Deepika N, Yata Praveen K, Devi CS, Venkat Reddy P, Srishailam A, Satyanarayana S, Synthesis, characterization, and DNA binding, photocleavage, cytotoxicity, cellular uptake, apoptosis, and on-off light switching studies of Ru(II) mixed-ligand complexes containing 7-fluorodipyrido[3,2-*a*:2',3'-*c*]phenazine. *J Biol Inorg Chem*, 2013; 18; 751–766.
 - Srishailam A, Yata PK, Nazar MDG, Venkat Reddy P, Deepika N, Veerababu N, Satyanarayanan S. Synthesis, DNA-binding, Cytotoxicity, Photo Cleavage, Antimicrobial and Docking Studies of Ru(II) Polypyridyl Complexes. *J Fluoresc*, 2013; 23; 897–908.
 - Sullivan BP, Salmon DJ, Meyer TJ. Mixed phosphine 2, 2'-bipyridine complexes of ruthenium. *Inorg Chem*, 1978; 17: 3334–3341.
 - Wolfe A, Shimer GH, Meehan T. Polycyclic aromatic hydrocarbons physically intercalate into duplex regions of denatured DNA. *Biochemistry*, 1987; 26: 6392–6396.
 - Chaires JB, Dattagupta N, Crothers DM. Studies on interaction of anthracycline antibiotics and

- deoxyribonucleic acid: equilibrium binding studies on interaction of daunomycin with deoxyribonucleic acid. *Biochemistry*, 1982; 21: 3927–32.
30. Satyanarayana S, Dabrowiak JC, Chaires JB. Tris(phenanthroline)ruthenium(II) enantiomer interactions with DNA: Mode and specificity of binding. *Biochemistry*, 1993; 32: 2573–2584.
 31. Drew WL, Barry AL, Toole RO, Sherris JC. Reliability of the Kirby-Bauer disc diffusion method for detecting methicillin-resistant strains of *Staphylococcus aureus*. *Appl Microbiol*, 1972; 24: 240–7.
 32. Mosmann T. Rapid colorimetric assay for cellular growth and survival: application to proliferation and cytotoxicity assays. *J Immunol Methods*, 1983; 65: 55–63.
 33. Vilar S, Cozza G, Moro S, Medicinal chemistry and the molecular operating environment (MOE): application of QSAR and molecular docking to drug discovery. *Curr Top Med Chem*, 2008; 8: 1555–1572.
 34. Pyle A. M., Rehmann J. P., Meshoyrer R., Kumar C. V., Turro N. J., Barton J. K. Mixed-ligand complexes of ruthenium(II): factors governing binding to DNA. *J Am Chem Soc*, 1989; 111: 3051–3058.
 35. Haga MA. Synthesis and protonation-deprotonation reactions of ruthenium(II) complexes containing 2, 2'-bibenzimidazole and related ligands. *Inorg Chim Acta*, 1983; 75: 29–35.
 36. Joseph R, Lakowicz GW. Quenching of fluorescence by oxygen. Probe for structural fluctuations in macromolecules. *Biochemistry*, 1973; 12: 4161–4170.
 37. Lakowicz JR. Principles of Fluorescence spectroscopy. Plenum Press York, 1983.
 38. Satyanarayana S, Dabrowiak JC, Chaires JB. Neither. DELTA.- nor. LAMBDA.-tris(phenanthroline)ruthenium(II) binds to DNA by classical intercalation. *Biochemistry*, 1992; 31: 9319–9324.
 39. Basile LA, Barton JK. Design of a double-stranded DNA cleaving agent with two polyamine metal-binding arms: Ru(DIP)₂Macron⁺. *J Am Chem Soc*, 1987; 109: 7548–7550.
 40. Kishikawa H, Jiang YP, Goodismam J, Dabrowiak JC. Coupled kinetic analysis of cleavage of DNA by esperamicin and calicheamicin. *J Am Chem Soc*, 1991; 113: 5434–5440